Journal of Coastal Research	11	1	154–167	Fort Lauderdale, Florida	Winter 1995

Eddy Formation Behind a Coastal Headland

Peter A. Davies†, Julie M. Dakin† and Roger A. Falconer‡

†Department of Civil Engineering
The University
Dundee DD1 4HN, U.K.

‡Department of Civil Engineering
The University
Bradford BD7 1DP, U.K.

ABSTRACT

DAVIES, P.A.; DAKIN, J.M., and FALCONER, R.A., 1995. Eddy formation behind a coastal headland. *Journal of Coastal Research*, 11(1), 154–167. Fort Lauderdale (Florida), ISSN 0749-0208.

The two-dimensional steady flow of a coastal flow past a headland has been considered. Results from a numerical model are presented to show the transient and steady state flow structures downstream of the headland, for a range of external parameters. It is demonstrated that the flows are of two types. The first type, which is characterised by low values of the bottom friction parameter (M) and low values of the Froude number (Fr), shows deflection of the incident flow around the cape tip and attachment of the flow to the rear face of the headland. For higher values of M and Fr, separation of the flow occurs at the tip of the headland and an attached eddy is generated downstream. Eddy shedding is not observed. The results show that the size of the attached eddy and the vorticity distribution within it are controlled strongly by the value of M, though the maximum vorticity within the eddy depends only upon the incident flow velocity U and the horizontal dimension L of the obstruction. Evidence of oscillatory behaviour is detected during the transient adjustment phase of flow development, with the period of the oscillations being of the same order as vortex shedding periods for the same geometry.

ADDITIONAL INDEX WORDS: *Eddies, topographic effects, rotating flows, vorticity, coastal flows, capes, headlands.*

INTRODUCTION

There has been a recognition for many years that capes, islands, headlands, promontories and other topographic indentations can exert controlling influences upon the trajectories and dynamics of coastal currents. Recently-available high resolution remotely-sensed imagery from satellite (BERNSTEIN *et al.*, 1977; NISHIMURA *et al.*, 1984) and aircraft overflights (DAVIES and MOFOR, 1990) of coastal waters has illustrated this control clearly and has served to stimulate renewed interest in topographic interactions with coastal currents. The reasons for this interest lie principally in the relevance of the problem to water quality and coastal morphology. For example, closed attached eddies may form in the lee of capes, with consequent modifications to local distributions of sediment deposition (FERENTINOS and COLLINS, 1979, 1980) and trapping of pollutants, chemicals, nutrients and marine species (UDA, 1970; UDA and USHINO, 1958; EMERY, 1972; ALLDREDGE and HAMNER, 1980; HAMNER and HAURI, 1981; SIGNELL, 1989). In the engineering context, the formation of eddies downstream of headlands affects the placement of outfalls and other marine discharge structures in a crucial way. Effluent discharged into these zones becomes trapped within the closed circulations established by the flow. Additionally, the pattern of sediment movement and deposition behind the headland is controlled by the velocity field within the attached eddy; this has important practical consequences for the access to, and navigability of, these zones.

Under conditions in which eddies are shed by topographic obstructions rather than remaining attached, temporal variations of the above environmental parameters become important downstream. The reader is referred to the studies by PATTIARATCHI *et al.* (1986), FALCONER (1986), FALCONER *et al.* (1988), DAVIES *et al.* (1990) and DAVIES and MOFOR (1990) for further discussions on these matters.

For the practical reasons given above, it is important to model the flow in the lee of a headland in order to predict the structure of the trapped flow and understand the fluid dynamics of the interaction process. Thus far, no models have been developed to address this particular problem, so it is appropriate to begin with consideration of an idealised case which contains the essential elements of the interaction of a coastal current with a cape or headland. In the present modelling study, consideration is given to the homogeneous two-

93111 received 30 September 1993; accepted in revision 28 March 1994.

dimensional flow of a uniform current past an idealised triangular headland. The problem has been addressed by adapting an existing numerical model (FALCONER, 1976, 1986; FALCONER *et al.*, 1986) to the geometry under consideration. This model has already been employed with considerable success in cases of tidal flow in regions of complex lateral topography. For such cases and for the shallow water coastal configuration studied here, it is necessary to consider cases in which bottom friction plays an important role in the interaction and for which the Coriolis term is retained in the equations of motion. The inclusion of background rotation in the model becomes necessary whenever flows are considered as follows: (1) when the horizontal length scale of the topographic obstruction is sufficiently large, and/or (2) the characteristic velocity scale of the current is sufficiently small, for the local Coriolis acceleration associated with the background rotation of the Earth to play a significant dynamical role in the interaction of the topography with the flow. Formally, this occurs whenever the values of the Rossby number Ro and the Ekman number Ek (see below) are both significantly less than unity. A number of laboratory experiments (BOYER and DAVIES, 1982; DAVIES and BOYER, 1984; BOYER *et al.*, 1984; 1987a,b; BOYER and TAO, 1987; DAVIES *et al.*, 1991; CHABERT D'HIÈRES *et al.*, 1989, 1990) on topographic interactions in rotating fluids have been performed within these parameter regimes, where the effects of background rotation were dominant. Laboratory studies of homogeneous non-rotating flows past capes are limited to the qualitative investigations of MITSUYASU and HIRAKI (1969) and the more recent investigations by PULLIN and PERRY (1980) on starting vortices generated by triangular capes. Recent experiments (DAVIES *et al.*, 1990) have also been reported in which the effects of density stratification upon such non-rotating cape flows have been studied. Theoretical studies of rotating flows past blunt headlands are restricted to the investigations of SIGNELL (1989), FREELAND (1990) and VERRON *et al.* (1991). Most of these studies are concerned only with flows in geostrophic or quasigeostrophic balance.

THE NUMERICAL MODEL

Physical System

Figure 1 shows the physical system under consideration. At time t = 0, the horizontal flow of a homogeneous fluid of undisturbed depth H is initiated upstream of a cape of depth H, base width W and maximum horizontal extent L. The cape is mounted on the side of a channel of width Y, rotating uniformly about a vertical axis with angular velocity f/2. The time-averaged mean velocity of the upstream undisturbed flow is U, and the bottom friction characteristics of the channel are represented by the (dimensional) Manning coefficient n (DOUGLAS *et al.*, 1985). The undisturbed and disturbed regions of the flow are assumed to be two dimensional in structure, the upper surface of the fluid is free, and the flow is bounded below by a horizontal solid surface.

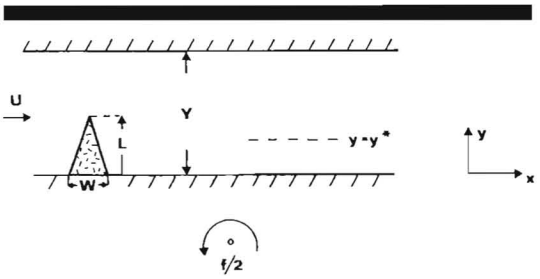

Figure 1. Plan view of the physical system under consideration.

Model Equations

Under the assumption of hydrostatic flow, the vertically-integrated equations of continuity and horizontal momentum may be written (FALCONER, 1976) in a Cartesian frame of reference (x, y, z) as

$$\partial\eta/\partial t + \partial(uH)/\partial x + \partial(vH)/\partial y = 0 \qquad (1)$$

and

$$\begin{aligned}\partial(uH)/\partial t &+ \beta\{\partial(u^2H)/\partial x + \partial(uvH)/\partial y\} \\ &- fvH + gH\partial\eta/\partial x + gn^2u|U|/H^{1/3} \\ &+ \epsilon\{2\partial^2(uH)/\partial x^2 + \partial^2(uH)/\partial y^2 \\ &\quad + \partial^2(vH)/\partial x\partial y\} = 0 \qquad (2)\end{aligned}$$

$$\begin{aligned}\partial(vH)\partial t &+ \beta\{\partial(uvH)/\partial x + \partial(v^2H)/\partial y\} \\ &+ fuH + gH\partial\eta/\partial y + gn^2v|U|/H^{1/3} \\ &+ \epsilon\{\partial^2(vH)\partial x^2 + 2\partial^2(vH)/\partial y^2 \\ &\quad + \partial^2(uH)/\partial x\partial y\} = 0 \qquad (3)\end{aligned}$$

respectively. Here, u and v are the depth-mean velocity components in the (x) down- and (y) cross stream directions, respectively, g = (0, 0, −g) is

the acceleration due to gravity, and η is the elevation of the free surface above the mean depth H. The quantity β is a correction factor (DOUGLAS *et al.*, 1985) for the non-uniformity of the vertical velocity profile and ϵ is the depth-averaged eddy viscosity of the fluid. If a seventh power velocity profile is assumed, the terms β and ϵ can be assigned values 1.016 and $1.167gn^2H^{2/3}U$, respectively (FALCONER, 1985).

The governing equations are solved using an alternating direction implicit (ADI) finite difference scheme, with all terms being fully centred in both space and time by iteration. Full details of the difference scheme are given in FALCONER *et al.* (1986, 1988). The impermeability (*i.e.*, zero normal velocity) and no-slip boundary conditions were applied along solid boundaries, and at the incoming open boundary, a constant velocity u = (U, 0, 0) was imposed. This upstream velocity was introduced smoothly as u = U sin Nt, over N = 100 time steps. The downstream open boundary condition was posed in terms of no cross stream variation in the downstream velocity (*i.e.*, u = U and du/dy = 0 at x = X). In addition, a Coriolis or water surface slope

$$\partial\eta/\partial y = -fU/g \tag{4}$$

was introduced at the downstream open boundary in order to prevent recirculation there (FALCONER, 1985; MARDAPITTA-HADJIPANDELI, 1985).

For convenience, the triangular cape was represented as a stepped edge, and the grid spacing (Δx) was related to the other dimensions of the problem as $L = 4(\Delta x)$, $X = 73(\Delta x)$, and $Y = 20(\Delta x)$. Experiments were performed to investigate the effects upon the flow of increasing the above upstream and downstream distances from the cape tip, but no such effects were detectable.

RESULTS

Dimensionless Parameters

It is convenient to view the results of the experiments in terms of the relevant non-dimensional parameters controlling the flow. A set of such parameters may be formed from the following dimensionless dynamical groupings:

$Ro = U/fL$, the Rossby number,
$Fr = U/(gH)^{1/2}$, the Froude number, and
$M = H^{4/3}/gLn^2$, the friction parameter,

together with the geometrical parameters L/H, L/W, and L/Y. (Note that the parameter M expresses the relative importance of the advective and bottom friction terms in the equation of motion.) For cases in which the surface elevation is small ($\eta \ll H$), the magnitude of the bottom friction acceleration F is defined in terms of the bottom stress τ and the depth H as

$$|F| = \tau/\rho H.$$

The magnitude of the stress τ may be written in terms of a drag coefficient C_D as

$$|\tau| = \rho C_D U^2 \tag{5}$$

where C_D is given (FALCONER, 1986) by

$$C_D = gn^2H^{-1/3} \tag{6}$$

Thus, with M defined as

$$M = |u \cdot u|/|F| L$$

it is easily shown that M takes the value $M = H^{4/3}/gn^2L$ listed above.

Finally, it is noted that the derived parameter Ek* (the equivalent Ekman number (PATTIARATCHI *et al.*, 1986)) is of relevance to the interpretation of some of the results. Here, Ek* is defined as

$$Ek^* = (\tau/\rho H)/(fU) \tag{7}$$

or

$$Ek^* = gn^2U/fH^{4/3} = Ro/M, \tag{8}$$

using the expressions above. In the experiments presented herein, the ranges of the above parameters were varied within the following limits:

$$0 \le Ro^{-1} \le 8$$
$$4.5 \times 10^{-3} \le Fr \le 1.1 \times 10^{-1}$$
$$0.3 \le M \le 200$$
$$0 \le (E_k^*)^{-1} \le 1.6 \times 10^3$$

Note that in the non-rotating cases, M always exceeded Fr by at least one order of magnitude, indicating the relative weakness in the flow of inertial accelerations. In the experiments, variations in the flow conditions were effected by changes in U, n and f; the geometry of the channel and the cape and the fluid depth H were kept constant throughout.

Qualitative Results

A number of experiments were conducted to investigate the development with time of the streamline and vorticity fields. Such experiments enabled the forms of the transient and fully-de-

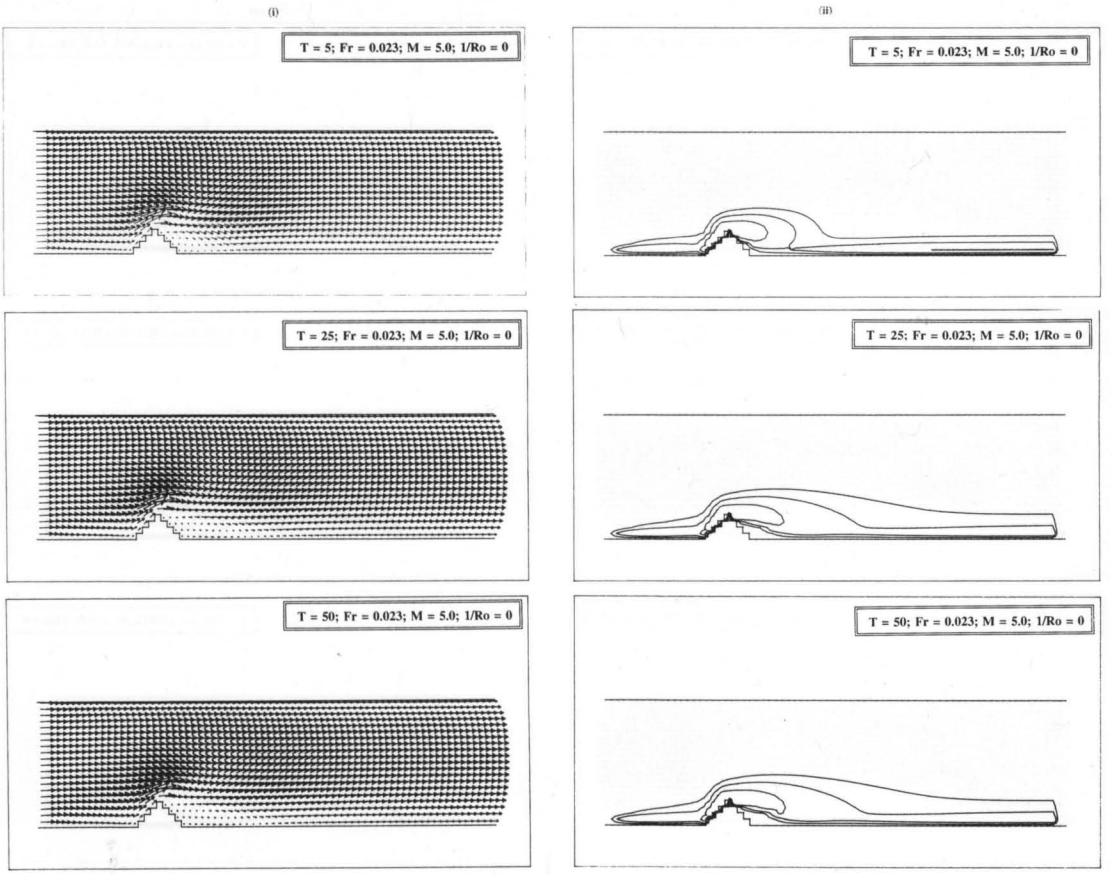

Figure 2a. Plan view plots showing the transient development of (i) velocity and (ii) vorticity patterns for parameter values shown. In this and all subsequent figures, velocity vectors scaled with incident flow velocity; dimensionless vorticity contours (a) 0.3, (b) 0.6, and (c) 1.2.

veloped flows to be determined, and allowed estimates to be made of the times taken for steady flow patterns to become established. Representative examples from these experiments are shown in Figure 2.

In both cases, the approach to a final steady state flow can be seen clearly. A comparison between the first two sequences (Figures 2a and b) reveals that, for a constant value of Fr, the characteristic adjustment time to the final steady state is determined strongly by the value of the friction parameter M. The effects of Fr upon the transient flow development can also be gauged by comparing the vorticity fields for Figures 2a and c, both of which are for the same value of M. In these cases the effects upon the flow of increasing Fr are not significant because of the dominating effects of friction, and the transient development of the flow depends only upon the value of M.

As indicated above, it is of interest to note that for certain parameter combinations the flow was observed to develop significant oscillatory characteristics (see Figure 3) before finally reaching a steady fully-developed state. For such cases, there are periodic fluctuations with time, in the size and form of the attached eddy in the lee of the cape and the spatial vorticity distributions within the eddy. Though such flow behaviour might be regarded as being indicative of incipient shedding of the attached eddy, no evidence of shedding was detected within the parameter ranges considered.

Figure 4 illustrates examples of the two steady forms which constitute the principal stable flow types observed for the range of parameters con-

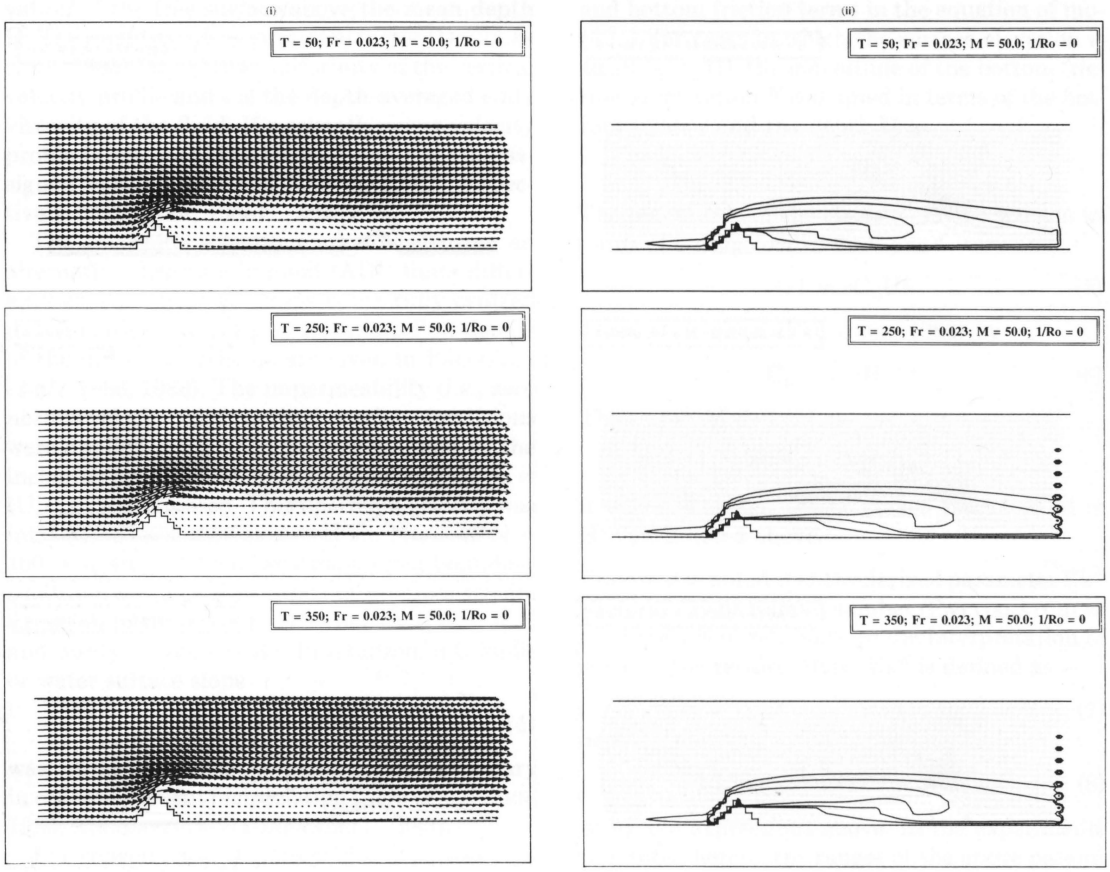

Figure 2b. Continued.

sidered. That is, attached flow (Figure 4a) and attached eddy flow (Figure 4b).

It is found that the transition between the two steady flow types is determined essentially by the value of the friction parameter M. For low values of M, the flow is characterised at all values of Fr by the pattern shown in Figure 4a, with little evidence of eddies forming in the lee of the cape. Instead, the incident streamlines close to the cape are deflected around the tip and follow the contours of the rear face of the cape before returning to their initial lateral locations. The flow has approximate up- and downstream symmetry within this regime. For intermediate and high values of M, separation occurs at the tip of the cape and a region of downstream attached eddies is formed in which the flow recirculates between the rear face of the cape and the lateral wall of the channel (Figure 4b). Incident streamlines approaching the cape tip are deflected by the attached eddy region as they pass downstream.

For cases in which the significant oscillatory fluctuations in the flow pattern became apparent during the transient phase of development, it was possible to estimate the periods Θ of the fluctuations (and their dependence upon Fr and M). This was accomplished by monitoring the motions of identifiable features within the eddy streamline and vorticity fields, throughout a time sequence. It is convenient to normalise the period of the oscillation as $\Pi = L/U\Theta$, and to plot the variation of Π with Fr and M as shown in Figure 5. The plotted data reveal that the values of Π decrease with decreasing Fr. The decrease of Π with Fr seems to be independent of the value of M.

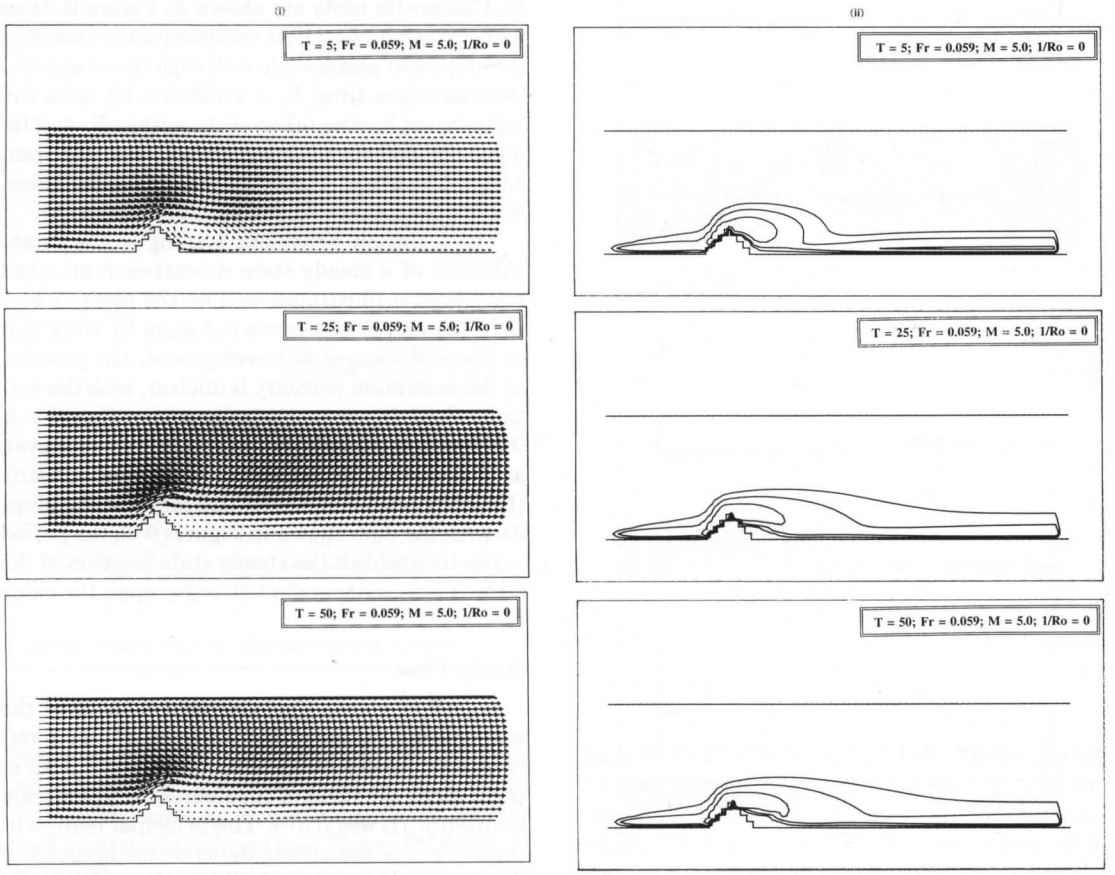

Figure 2c. Continued.

Quantitative Measurements

Flow Observables

In order to assess quantitatively the temporal and spatial effects upon the flow of changes in the values of the dynamical parameters Ro, Fr and M, it is necessary to identify characteristic observable quantities in the streamline and vorticity patterns with which to monitor such effects. For the present study, it has been found useful to consider (i) the length λ of the attached eddy region, (ii) the distance γ from the cape tip to the position of maximum value of the vertical component of the vorticity within the eddy, and (iii) the magnitude $(\Phi)_{max}$* of the vertical component of the maximum vorticity itself, as the three most significant quantitative observables. In all cases, the quantities were measured along a reference cross stream line y/L = y*/L from the channel wall (see Figure 1), with the value of y* being chosen to give (i) a realistic representation of the flow and (ii) maximum discrimination between different flow cases. The observables were expressed in dimensionless form, with the quantities L and U/L being used to normalise lengths and vorticities respectively.

Transient Flow

Figures 6, 7 and 8 show the variations of λ, γ and $(\Phi)_{max}$* with the advective time Ut/L, for two different values of M. The plots confirm the previous qualitative conclusions regarding the sensitivity of the flow adjustment time to the value of M during the transient phase. A scaling analysis of the equations of motion suggests that the relevant dimensional adjustment time for cases in

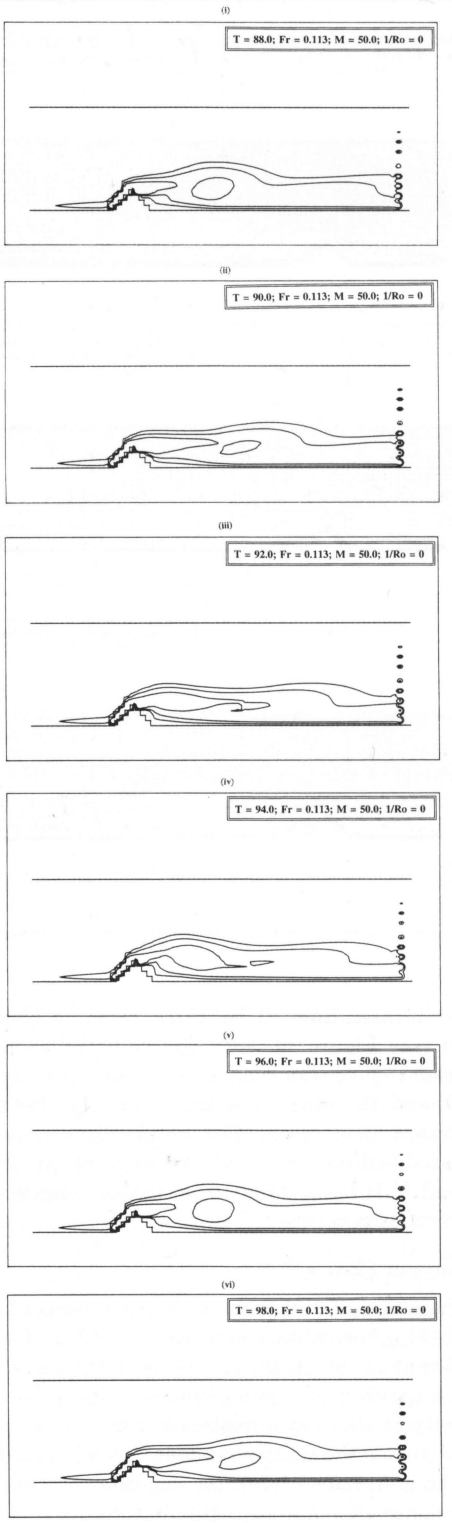

which the flow is dominated by friction is t = ML/U. Composite plots are shown in Figure 9, from where it can be seen that the data for the transient development phase scale well with the associated dimensionless time $T_a = (1/M)(Ut/L)$, with full adjustment having taken place within $T_a \approx 6$ for all of the non-rotating cases. Note that the transient adjustment processes are relatively insensitive to the values of the Froude number Fr.

The transient behaviour leading to the establishment of a steady state downstream attached eddy field is illustrated well by the plots of $\Phi(y/L, T, M)$ versus x/L shown in Figure 10. Note that in the early stages of development, the position of the maximum vorticity is unclear, with the vorticity decaying monotonically with x for all $y \geq 0.375$ as the eddy form is established. However, as T increases, a position of maximum vorticity (the eddy centre) is clearly indicated on the plots. As with the data shown in Figures 6–8, the period taken to establish the steady state location of the eddy centre is dependent strongly upon the value of M.

Steady Flow

Figure 11 shows the variations with M of the steady state values of λ, γ and $(\Phi)_{max}^*$, for a reference y/L and a range of values of Fr. For all of these plots, the value of the reference cross stream location y^*/L was 0.375. The principal feature of these plots is the strong dependence upon M of the two distances λ and γ. The insensitivity of these quantities to changes in the value of Fr is seen very clearly when these data are replotted against Fr for several different values of M (see Figure 12). The increases in λ and γ with increasing M are nonlinear.

Figure 11 illustrates that $(\Phi)_{max}^*$ varies only weakly with M over the full range of Fr. Indeed, except for cases where M is very low ($\ln M \leq 1$) and frictional effects dominate the flow, the value of the maximum vorticity is essentially constant at around unity. Thus, Figure 11 shows that, for the reference y/L, the maximum vorticity within the attached eddy continues to scale with the advective scale U/L over most of the range of M, though the vorticity produced at the cape tip is distributed over a successively larger area as M

←

Figure 3. Plan view plots showing oscillatory behaviour in velocity and vorticity fields for parameter values shown.

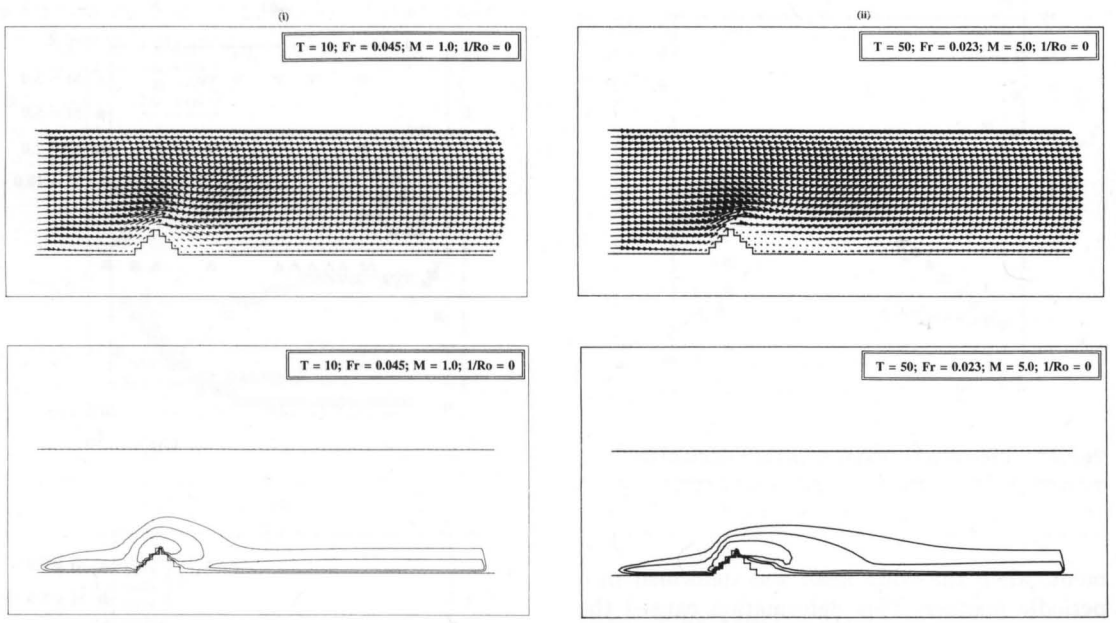

Figure 4. Steady state velocity and vorticity patterns for (i) attached and (ii) attached eddy flow types. Parameter values as shown.

increases. For the lower values of M, there are indications that the dissipation of vorticity by bottom friction is no longer insignificant, and the peak vorticity is reduced (see Figure 13) from the essentially constant value it has over much of the M range. It should be noted that the reference cross stream location y*/L used for comparing the different flow patterns did not always pass through the grid point corresponding to the centre of the eddy and/or the position of maximum vorticity within the eddy. However, the error involved in this misalignment was significant only during the oscillatory phase of the transient flow develop-

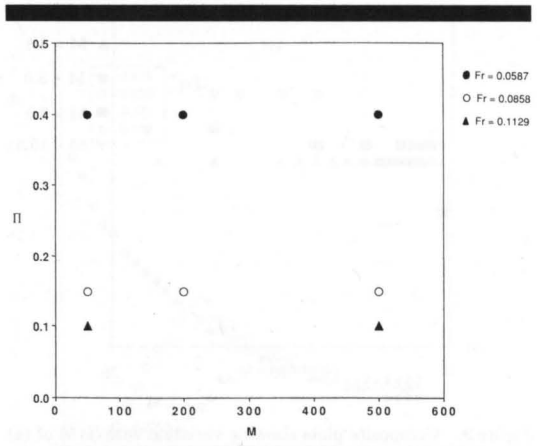

Figure 5. Plot of $\Pi = L/U\Theta$ versus M for Fr values shown. See text for explanation.

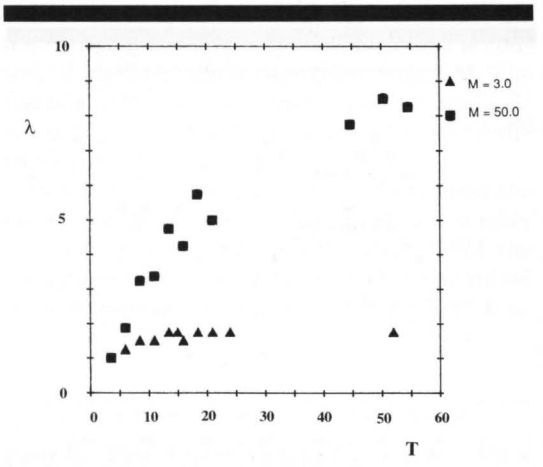

Figure 6. Plot of λ versus T for Fr = 2.26×10^{-1} and M = (a) 3.0 and (b) 50.0.

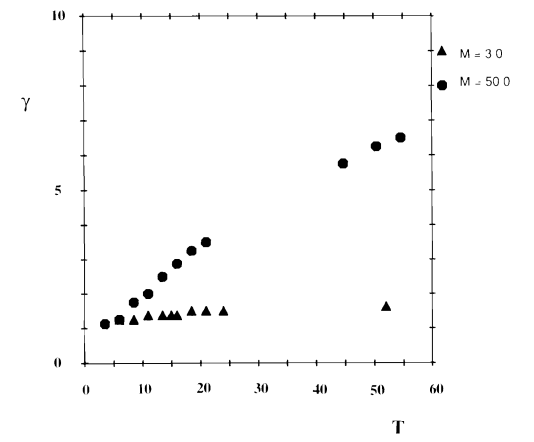

Figure 7. Legend as for Figure 6, except λ replaced by γ.

ment, when the eddy itself was deformed in a periodic manner. This deformation caused the centre of the eddy, and the position of maximum vorticity within it, to fluctuate periodically in the cross stream direction. During the steady state phase, the cross stream migrations of the eddy centre and the position of maximum vorticity were not significant, and the values of the flow observables obtained from y*/L = 0.375 gave satisfactory representations of the flow behaviour. This property is confirmed by inspection of the flow and vorticity patterns shown earlier in Figures 2 and 4.

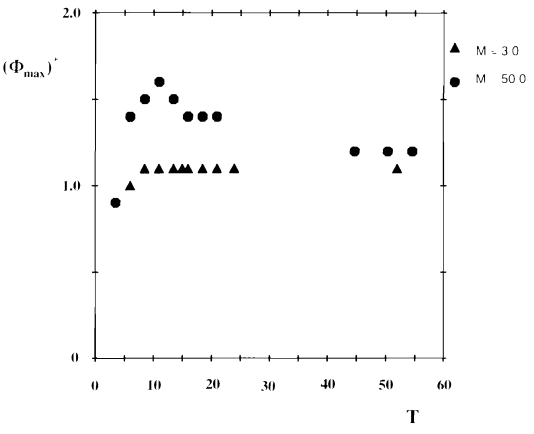

Figure 8. Legend as for Figure 6, except λ replaced by $(\Phi)_{max}$*.

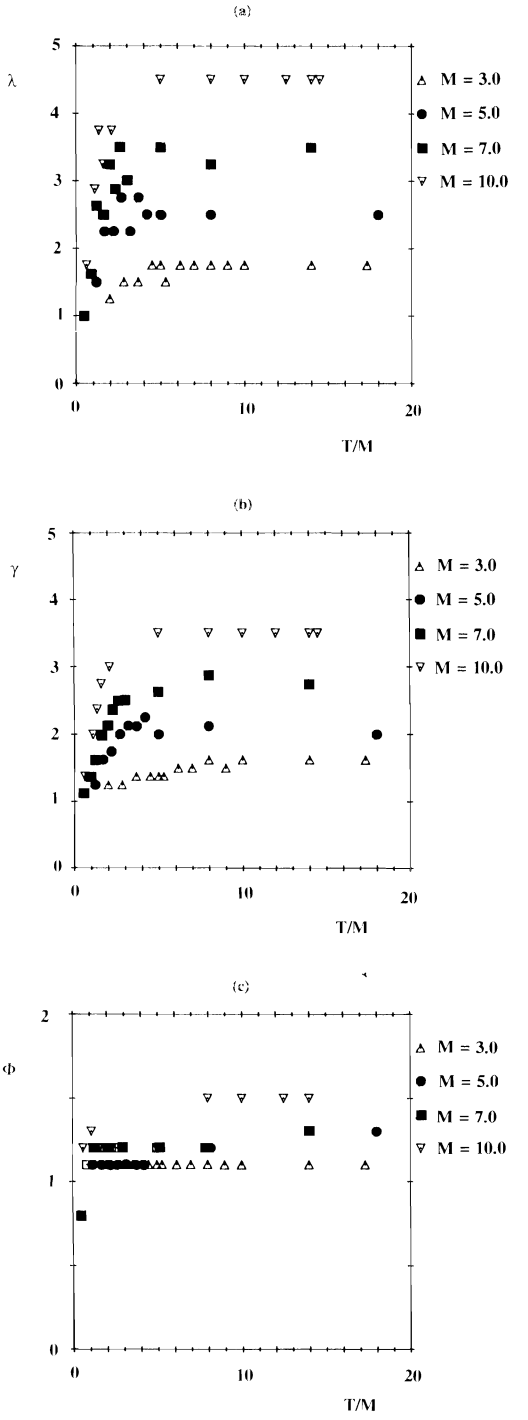

Figure 9. Composite plots showing variation with T/M of (a) λ, (b) γ, and (c) $(\Phi)_{max}$*, for $Ro^{-1} = 0$, Fr = 2.26 × 10^{-2} and M values shown.

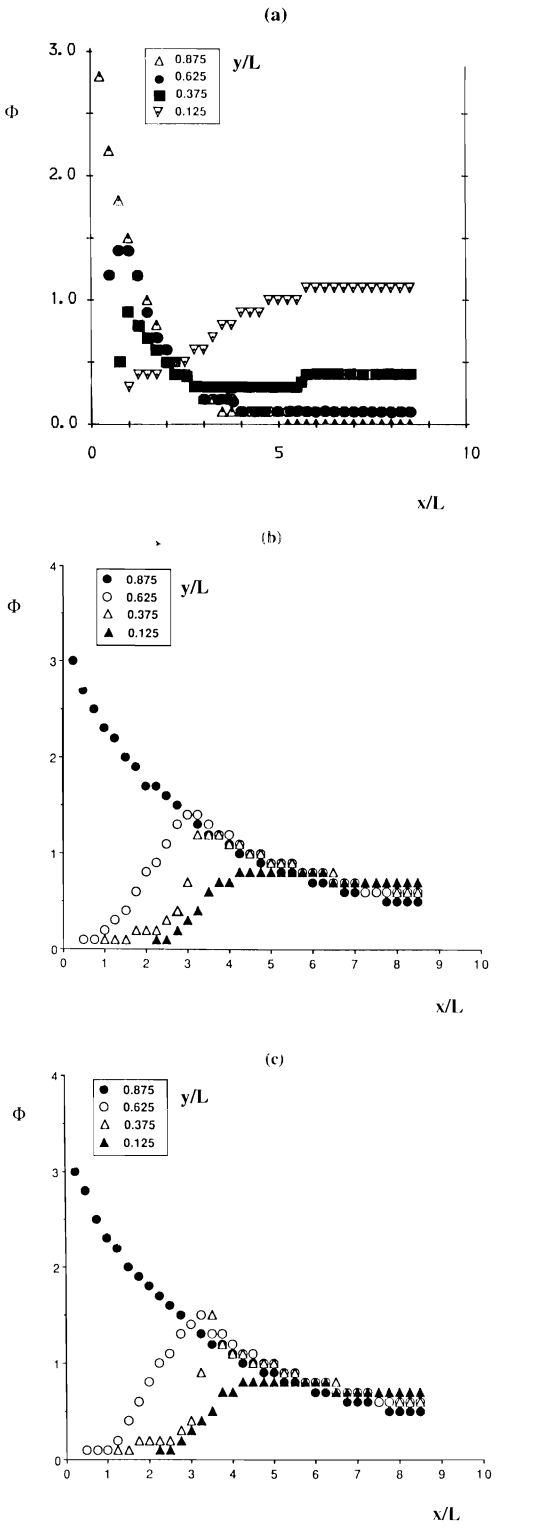

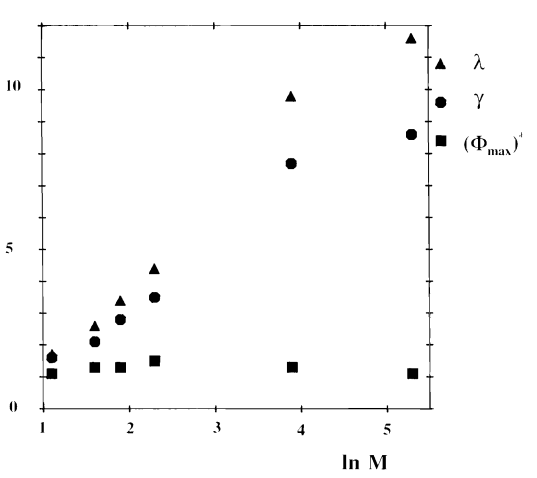

Figure 11. Plots of steady state value of λ, γ and $(\Phi)_{max}$* versus ln M for Fr = 2.26 × 10 $^{-1}$.

Effects of Background Rotation

The effects of increasing the value of Ro^{-1} (equivalent to increasing the background rotation parameter f while holding all other quantities constant) can be gauged by the typical plots shown in Figures 13 and 14. In Figure 13 the velocity and vorticity patterns are compared for non-rotating and rotating cases, under otherwise identical conditions. Such plots show that the effects of rotation upon the flow are insignificant, with the velocity and vorticity patterns in the two cases being qualitatively and quantitatively identical. As illustrated by the earlier measurements for the non-rotating flows, the flow development is controlled wholly by the bottom friction term M. The Coriolis and advective time scales f^{-1} and L/U respectively are both significantly less than the frictional time scale ML/U.

In Figure 14 the quantitative effects upon the downstream structure of the steady state eddy vorticity field of increasing the strength of the background rotation can be seen. Here the values of all parameters except f have been kept con-

←

Figure 10. Plots of Φ versus x/L for Ro $^{-1}$ = 0, Fr = 2.26 × 10^{-2}, M = 10.0 and T = (a) 3.5, (b) 50.0 and (c) 70.0 and y/L values shown.

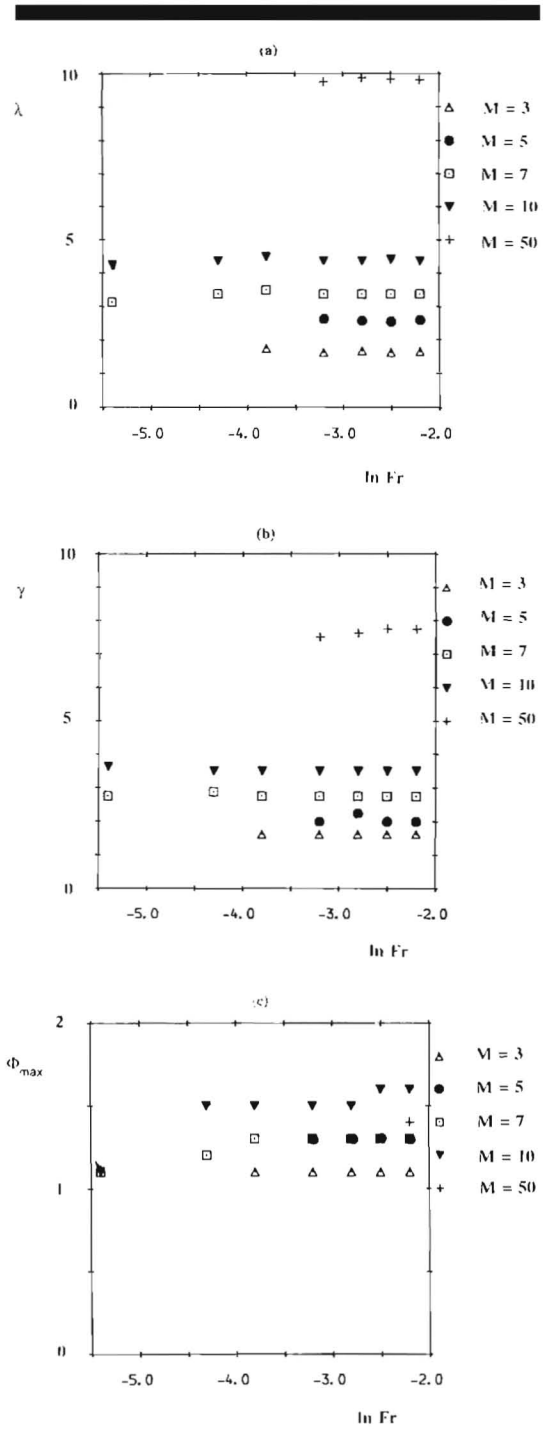

Figure 12. Plots versus Fr of steady-state values of (a) λ, (b) γ and (c) $(\Phi)_{max}$*, for M values shown.

stant. As in the previous figure (Figure 13), the influence of the background rotation upon the vorticity distribution within the attached eddy is insignificant, because of the dominance of the bottom friction.

SUMMARY AND DISCUSSION

The experiments have shown that numerically-stable solutions can be found for weakly-rotating flows in which the effects of bottom friction are dominant; and within the parameter ranges of the experiments, the flow can take one of two main forms. For low values of Fr and M, the flow is deflected around the tip of the cape to continue downstream without forming a closed circulation in the lee of the cape. For higher values of Fr and M, separation occurs at the tip and an attached eddy is generated between the lee face of the cape and the adjacent channel wall. The size and structure of the attached eddy are determined primarily by the value of the friction parameter M, with the eddy length and the position of maximum vorticity within the eddy both increasing rapidly with increasing M. The insensitivity of both of these quantities to the value of Fr is evidently due to the relative weakness of the inertial acceleration with respect to other terms in the equation of motion, even for the lowest values of M. Indeed, it has been noted earlier that the values of Fr for every case were always at least one order of magnitude less than those of M.

In all cases in which closed attached eddies were observed in the lee of the cape, the maximum vorticity within the eddy remained essentially constant over much of the range of M, except for the lowest values of M where dissipation of vorticity by bottom friction became a dominant process. Throughout the range of M, the overall shape of the flow and vorticity patterns changed relatively little, except for the lengthening in the eddy and the accompanying downstream shift in the eddy centre which occurred with increasing M. This behaviour, coupled with the relative constancy of $(\Phi)_{max}$* over the same range of M, indicates a gradual redistribution of the normalised vorticity within the eddy as M increases.

The domination of frictional effects in the model solutions is confirmed by the influence of M upon the transient behaviour of the flow and vorticity fields. Specifically, it has been shown that the adjustment time typifying the achievement of steady state conditions is of order ML/U, a time

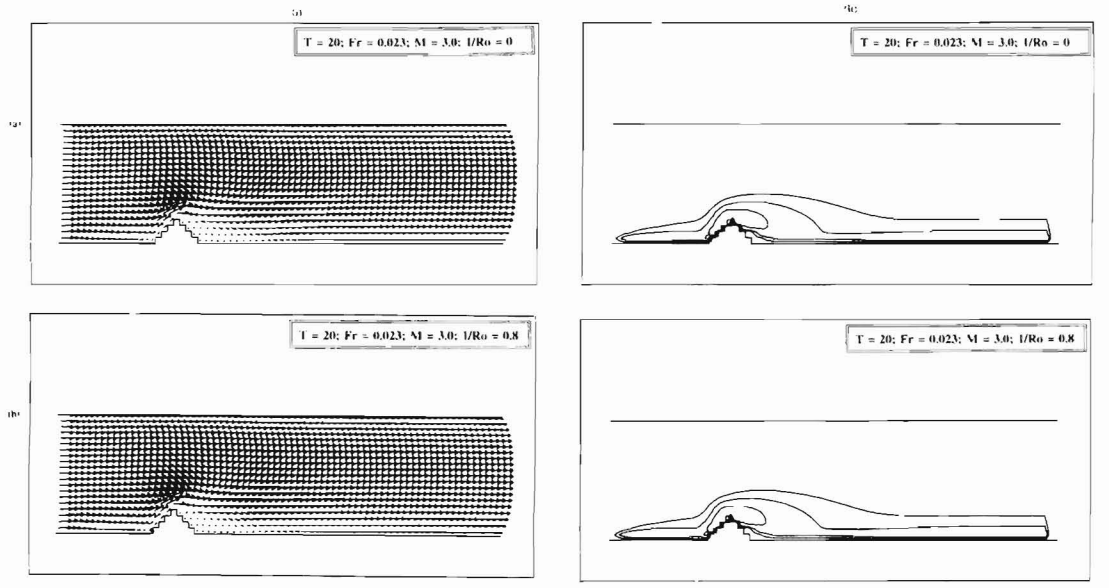

Figure 13. Plan view steady-state (i) velocity and (ii) vorticity fields for Fr = 2.26 × 10 $^{-2}$, M = 3.0 and Ro $^{-1}$ = (a) 0, (b) 0.8.

scale at least one order of magnitude greater than the other two time scales f^{-1} and L/U in the problem. This disparity in time scales evidently explains the weak effects upon all aspects of the flow development of both Fr and (especially) Ro, for cases (U/ML ≤ f ≤ U/L) investigated here. That is, for rotating flow cases corresponding to high friction and/or high Rossby number combinations.

The occurrence of oscillatory behaviour in the flow and vorticity fields during the adjustment to steady state may be regarded as an indication of incipient eddy shedding by the cape, particularly since the frequencies of the oscillations were comparable with typical eddy shedding frequencies measured (DAVIES *et al.*, 1990) in the laboratory for two-dimensional cape flows. It is somewhat surprising, therefore, that shedding was not observed in the flows for which the values of M were much greater than unity. The absence of the shedding phenomenon is evidently associated with the dominant damping exerted by the frictional terms in the equations of motion, for all flow conditions investigated.

The Manning coefficients considered lay within the range 0.000452 to 0.08245, (*i.e.*, 0.3 ≤ M ≤ 10,000), though the excessive integration time required (≈6 ML/U) precluded full coverage of the steady state flows at the upper limit of the range. Note that for estuaries and coastal waters, the bottom friction coefficient C_D is typically attributed (PATTIARATCHI *et al.*, 1986) a value of 0.0025, which, for a typical depth of, say 30 m, gives a value of n of approximately 0.028. Thus, for a typical case of a cape of extent 1 km in a mid-latitude coastal flow of U ≈ 1 m s^{-1} and a depth of, say 20 m, typical values of Fr, M and Ro for such cases (*i.e.*, Fr ≈ 6 × 10 $^{-2}$; M ≈ 4: Ro ≈ 3) lie well within the parameter ranges considered above. This indicates that for such cases, the principal component control upon the flow will be exerted by the friction term in the equation of motion. Such a control is most likely to be relaxed when water depths are much greater and current velocities are more vigorous than the values cited above. Note also that the dimensional friction time scale 6ML/U for full flow establishment will often be significantly longer than a typical tidal period (say 6 hours), for the typical values of U, L and M given above. This implies that for many coastal situations the observed flow at any stage of the tidal cycle may have a structure quite different from the flow which would result if the same flow velocity were imposed for much longer times.

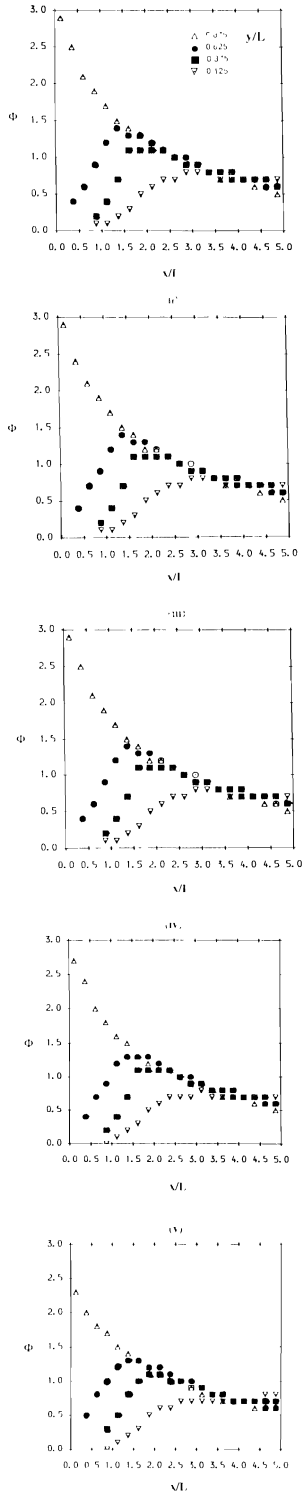

ACKNOWLEDGEMENTS

Financial support for this investigation was provided by the Natural Environment Research Council (through the award of a Ph.D. studentship to J.M.D.) and NATO Scientific Affairs Division (Research Grant CRG 901048). The authors acknowledge this support with gratitude. In addition, they thank P. Besley, D.L. Boyer and G. Chabert d'Hières for useful discussions.

LITERATURE CITED

ALLDREDGE, A.L. and HAMNER, W.M., 1980. Recurring aggregation of zooplankton by a tidal current. *Estuarine Coastal and Marine Science,* 10, 31–37.

BERNSTEIN, R.L.; BREAKER, L., and WHRITNER, R., 1977. California current eddy formation: Ship, air and satellite results. *Science,* 195, 353–359.

BOYER, D.L. and DAVIES, P.A., 1982. Flow past a circular cylinder on a beta plane. *Philosophical Transactions of the Royal Society of London,* A306, 533–566.

BOYER, D.L.; KMETZ, M.L.; SMATHERS, L.; CHABERT D'HIERES, G., and DIDELLE, H., 1984. Rotating open channel flow past right circular cylinders. *Geophysical and Astrophysical Fluid Dynamics,* 30, 271–304.

BOYER, D.L.; CHEN, R.; CHABERT D'HIERES, G., and DIDELLE, H., 1987a. On the formation and shedding of vortices from side wall mounted obstacles in rotating systems. *Dynamics of Atmospheres and Oceans,* 11, 59–86.

BOYER, D.L.; DAVIES, P.A.; HOLLAND, W.R.; BIOLLEY, F., and HONJI, H., 1987b. Stratified rotating flow over and around isolated three-dimensional topography. *Philosophical Transactions of the Royal Society of London,* 322, 213–241.

BOYER, D.L. and TAO, L., 1987. On the motion of linearly stratified rotating fluids past capes. *Journal of Fluid Mechanics,* 180, 429–449.

CHABERT D'HIERES, G.; DAVIES, P.A., and DIDELLE, H., 1989. A laboratory study of the lift forces on a moving solid obstacle in a rotating fluid. *Dynamics of Atmospheres and Oceans,* 13, 47–77.

CHABERT D'HIERES, G.; DAVIES, P.A., and DIDELLE, H., 1990. Experimental studies of lift and drag forces upon cylindrical obstacles in homogeneous, rapidly-rotating fluids. *Dynamics of Atmospheres and Oceans,* 15, 87–116.

DAVIES, P.A. and BOYER, D.L., 1984. Quasi-geostrophic flow past isolated obstacles. *Rivista di Meteorologia Aeronautica,* 44, 265–275.

DAVIES, P.A.; BOYER, D.L.; TAO, L., AND DAVIS, R.G., 1991. Stratified rotating flow past isolated obstacles. *In:* LIST, E.J. and JIRKA, G.H. (eds.), *Stratified Flows.* New York: American Society of Mechanical Engineers, pp. 228–237.

←

Figure 14. Plots of Φ versus x/L and y/L for Fr = 2.26 × 10 $^{-2}$, M = 5.0, T = 18.5, and Ro $^{-1}$ = (i) 0, (ii) 0.1, (iii) 0.2, (iv) 0.4, and (v) 0.8.

DAVIES, P.A. and MOFOR, L.A., 1990. Observations of flow separation by an isolated island. *International Journal of Remote Sensing,* 11(5), 767–782.

DAVIES, P.A.; BESLEY, P., and BOYER, D.L., 1990. An experimental study of flow past a cape in a linearly stratified fluid. *Dynamics of Atmospheres and Oceans,* 14, 497–528.

DOUGLAS, J.F.; GASORIEK, J.M., and SWAFFIELD, J.A., 1985. *Fluid Mechanics.* London: Pitman, pp. 1–746.

EMERY, R.A., 1972. Eddy formation from an oceanic island: Ecological effects. *Caribbean Journal of Science,* 12, 121–128.

FALCONER, R.A., 1976. Mathematical Modelling of Jet-forced Circulation in Reservoirs and Harbours. Ph.D. Dissertation, London: University of London, U.K.

FALCONER, R.A., 1985. Residual currents in Port Talbot Harbour: A mathematical model study. *Proceedings of the Institution of Civil Engineers,* 79, 33–53.

FALCONER, R.A., 1986. Water quality simulation study of a natural harbor. *Journal of Waterway, Port, Coastal and Ocean Engineering,* 112, 15–34.

FALCONER, R.A.; WOLANSKI, E., and MARDAPITTA-HADJIPANDELI, L., 1986. Modelling tidal circulation in an island's wake. *Journal of Waterway, Port, Coastal and Ocean Engineering,* 112, 234–254.

FALCONER, R.A.; WOLANSKI, E., and MARDAPITTA-HADJIPANDELI, L., 1988. Discussion: Modelling tidal circulation in an island's wake. *Journal of Waterway, Port, Coastal and Ocean Engineering,* 114, 104–110.

FERENTINOS, G. and COLLINS, M.B., 1979. Tidally-induced secondary circulations and their associated sedimentation processes. *Journal of the Oceanographic Society of Japan,* 35, 65–74.

FERENTINOS, G. and COLLINS, M.B., 1980. Effects of shoreline irregularities on a rectilinear tidal current and their significance in sedimentation processes. *Journal of Sedimentary Petrology,* 50(4), 1081–1094.

FREELAND, H.J., 1990. The flow of a coastal current past a blunt headland. *Atmosphere-Ocean,* 28, 288–302.

HAMNER, W.M. and HAURI, I.R., 1981. Effects of islands mass: Water flow and plankton pattern around a reef in the Central Great Barrier Reef Lagoon. *Australian Limnology and Oceanography,* 26, 1084–1102.

MARDAPITTA-HADJIPANDELI, L., 1985. Numerical Modelling of Tide-induced Circulation. Ph.D. Dissertation, Birmingham: University of Birmingham, U.K.

MITSUYASU, A. and HIRAKI, N., 1969. Experimental investigation of the wake vortex behind the triangular obstacle protruding from the wall. *Proceedings of the 19th Japan National Congress of Applied Mechanics,* IV-II, 171–177.

NISHIMURA, T.; HATAKEYAMA, Y.; TANAKA, S., and MARUYASU, T., 1984. Kinetic study of self-propelled marine vortices based on remotely-sensed data. *In:* NIHOUL, J.C.J. (ed.), *Remote Sensing of Shelf Sea Hydrodynamics.* Amsterdam: Elsevier Scientific Publishing Co., pp. 69–105.

PATTIARATCHI, C.; JAMES, A., and COLLINS, M.B., 1986. Island wakes and headland eddies: A comparison between remotely-sensed data and laboratory experiments. *Journal of Geophysical Research,* 92, 783–794.

PULLIN, D.I. and PERRY, A.E., 1980. Some flow visualisation experiments on the starting vortex. *Journal of Fluid Dynamics,* 97, 239–255.

SIGNELL, R.P., 1989. Tidal Dynamics and Dispersion Around Coastal Headlands. Ph.D. Dissertation, Woods Hole Oceanographic Institution, U.S.A.

UDA, M., 1970. Fishery oceanography studies of frontal eddies and transport associated with the Kuroshio system, including the "subtropical countercurrent." *In:* MARR, C.J. (ed.), *The Kuroshio.* Honolulu: East West Centre Press, pp. 593–604.

UDA, M. and USHINO, M., 1958. Enrichment pattern resulting from eddy systems in relation to fishing grounds. *Journal of the Tokyo University of Fisheries,* 44, 105–129.

VERRON, J.; DAVIES, P.A., and DAKIN, J.M., 1991. Quasigeostrophic flow past a cape in a homogeneous fluid. *Fluid Dynamics Research,* 7, 1–22.